Sensors and Materials, Vol. 34, No. 11 (2022) 3933–3947
MYU Tokyo

S & M 3087

Three Types of Films from Liquid-phase-exfoliated Graphene for Use as Humidity Sensors and Respiration Monitors

Stevan Andrić,[1*] Tijana Tomašević-Ilić,[2] Lazar Rakočević,[3]
Dana Vasiljević-Radović,[1] and Marko Spasenović[1**]

[1]Center for Microelectronic Technologies, Institute of Chemistry, Technology and Metallurgy, National Institute of the Republic of Serbia, University of Belgrade, Njegoševa 12, Belgrade 11000, Serbia
[2]Institute of Physics Belgrade, University of Belgrade, Pregrevica 118, Belgrade 11080, Serbia
[3]INS Vinca, Department of Atomic Physics, University of Belgrade, Mike Petrovića Alasa 12–14, Belgrade 11351, Serbia

(Received August 27, 2022; accepted September 28, 2022)

Keywords: graphene, liquid-phase exfoliation, Langmuir–Blodgett assembly, humidity sensing, respiration monitoring

Measuring relative humidity is important for a myriad of industries, including production, agriculture, environmental monitoring, and medicine. Thin-film, fast-response sensors are particularly interesting for wearable applications, such as monitoring breathing. We report on humidity sensors made from graphene deposited as a thin film by the Langmuir–Blodgett (LB) method from three types of graphene in solution. We demonstrate humidity sensing and respiration monitoring from graphene made by bath sonication, probe sonication, and electrochemical exfoliation. We characterize the morphology and chemical composition of the three film types and compare their performance as sensors. We conclude that although all three types can be used for sensing, they each have their particular advantages and drawbacks.

1. Introduction

Knowledge of relative humidity (RH) is of crucial importance for various industries such as production, agriculture, environmental monitoring, and medicine.[1,2] Standard materials used for humidity sensing are based on metal and polymers;[2] however, insufficient transparency, thermal stability, flexibility, and response speed (in tens of seconds) have motivated research on other active materials for humidity sensing, especially in wearable applications.

Graphene has excellent mechanical and thermal stabilities, high transparency, and high flexibility, making it suitable for implementation in sensors such as humidity sensors.[3,4] Graphene obtained by chemical vapor deposition (CVD) and liquid-phase exfoliation (LPE) has been reported to have applications in humidity sensing and respiration monitoring, because water vapor is present in human breath.[5–9] The goal of graphene sensor research in general is to synthesize graphene films at a low cost while retaining the material's basic characteristics and achieving high reactivity to the sensed gas. One of the methods of synthesis is the formation of

*Corresponding author: e-mail: stevan@nanosys.ihtm.bg.ac.rs
**Corresponding author: e-mail: spasenovic@nanosys.ihtm.bg.ac.rs
https://doi.org/10.18494/SAM4092

ISSN 0914-4935
https://myukk.org/

graphene dispersions, which are obtained by LPE using several techniques, such as ultrasonic exfoliation, electrochemical exfoliation, ball milling, and high-shear mixing.[10] After obtaining a dispersion, one needs to deposit graphene from the solution onto a substrate to obtain solid-state graphene. For this purpose, Langmuir–Blodgett (LB) deposition, spin coating, or drop casting is used.[11] Both the LPE and LB methods are economical and efficient for synthesizing graphene films.[12]

In this paper we demonstrate three types of graphene humidity sensors, where graphene films were obtained from three types of LPE, with the LB method used to deposit graphene from a dispersion onto a solid substrate. The graphene films were tested as active humidity sensors as well as real-time respiration monitors. Their morphology and chemical composition were also characterized. We demonstrate that although there are differences in the chemical composition of the obtained graphene dispersions and in the morphology of the deposited films that contribute to different sensitivities to humidity, all three types of graphene exhibit humidity-sensing behavior, showing that LPE followed by the LB method is a robust approach for fabricating graphene-based humidity sensors.

In our previous work, we demonstrated ultrafast humidity sensing with bath-exfoliated graphene films.[13] The novelty of the current paper is a direct comparison of the sensor used in our previous work with other types of LPE graphene sensors. This is also, to the best of our knowledge, the first report of humidity sensing with commercially obtained electrochemically exfoliated graphene. First reports on in-lab electrochemically exfoliated graphene as a humidity sensor have appeared recently.[14]

2. Materials and Methods

2.1 Synthesis of graphene film

The first graphene dispersion was prepared by dispersing graphite powder (Sigma Aldrich, product no. 332461), with a concentration of 18 mg/ml in *N*-methyl-2-pyrrolidone (NMP) (Sigma Aldrich, product no. 328634). Such a dispersion was sonicated for 14 h in a low-power ultrasonic bath. After sonication, the obtained dispersion was centrifuged for 60 min at 3000 rpm to separate non-exfoliated graphite flakes, leaving only graphene flakes in the supernatant.[15] The second graphene dispersion was prepared using the same graphite powder with the same initial graphite concentration in aqueous sodium dodecylbenzenesulfonate (SDBS) (Sigma Aldrich, product no. 289957). This dispersion was sonicated for 6 h with an ultrasonic probe of 200 W power. Sonication was performed for 1 h, after which the solution was centrifuged for 90 min at 5000 rpm, then the sonication was continued for 5 h. The obtained dispersion was centrifuged for 90 min at 1500 rpm, whereby the non-exfoliated graphite flakes remained in the sediment and the supernatant contained exfoliated graphene flakes. The water-based graphene dispersion was transferred to NMP owing to its compatibility with LB deposition at an air/water interface.[10,12,16] For the transfer process, a mixture of 1 ml graphene dispersion in 11 ml isopropyl alcohol (IPA) was used. The mixture was centrifuged at 10000 rpm for 90 min to separate

graphene flakes of all sizes in the sediment. The supernatant was removed, and 2 ml cuvettes containing the sediment were refilled to the lines. The centrifugation step was repeated with the same parameters. After centrifugation, the described process was repeated one more time, for a total of three centrifugations. Instead of IPA, ~120 μm of NMP was poured into the final sediment, and all the dispersions were collected in one bottle. The third graphene dispersion was commercially obtained from Sixonia Tech GmbH (G-DISP-NMP-CSO-2+, Dresden, Germany). This dispersion was obtained by electrochemical exfoliation in NMP.

The three types of exfoliation have distinct advantages and disadvantages over each other. An ultrasonic bath with low-power ultrasound (around 30 W) is compatible with any solvent that is suitable for exfoliation, without the need to consider thermal stability. For instance, *N*-methyl-2-pyrrolidone (NMP) can be used as a solvent in exfoliation, from which homogeneous films can be directly deposited onto a liquid surface.[17] Exfoliation with an ultrasonic probe, on the other hand, is quick, powerful, and compatible with upscaling. Nevertheless, owing to the high power of exfoliation of up to 400 W, only thermally stable solvents can be used in exfoliation. After exfoliation, the graphene flakes must be transferred from the thermally stable solvent to one that can be used for LB deposition. The third dispersion is a commercially obtained graphene dispersion formed by electrochemical exfoliation. The advantage of using a commercial solution is that it removes the need for exfoliating in the laboratory where film formation and subsequent experiments are performed. However, the disadvantage is the lack of control over the exfoliation process and the final chemical composition of the material.

The LB method was used to produce the films from the above-described dispersions, in which a small amount, between 0.1 and 1 ml depending on the dispersion, of a graphene dispersion was carefully dripped in deionized water (18 MΩ/cm). The self-assembly of graphene flakes at the surface of the water resulted in the formation of a graphene film. This film was deposited on a suitable substrate.[12] Figure 1 shows photographs of all three graphene films deposited on a ceramic substrate with interdigitated gold electrodes (DropSens IDEAU200).

2.2 Characterization

To obtain the thickness of each graphene film without damaging the surface, UV–VIS (Thermo Scientific, Evolution 60) measurement in transmittance mode was used. Graphene was first assembled on transparent slides and the spectrum was recorded in the range from 300 to 700 nm with an emphasis on 660 nm, where the thickness was calculated from the optical transmittance. To measure the size of the graphene flakes and more closely examine the topography of the films, atomic force microscopy (AFM) was used with a scan area of 5 × 5 μm^2. For AFM, the films were deposited on a Si/SiO_2 substrate. Gwyddion software was used for the analysis of AFM images. For a clear understanding of the sensor mechanism during the interaction with humidity, namely, with water molecules, the chemical structure of graphene must be well known; therefore, X-ray photoelectron spectroscopy (XPS) was used. The analysis was performed with SPECS systems with an XP50M X-ray source for a Focus 500 X-ray monochromator and a PHOIBOS 100/150 analyzer. An AlKα source of 1486.74 eV at 12.5 kV

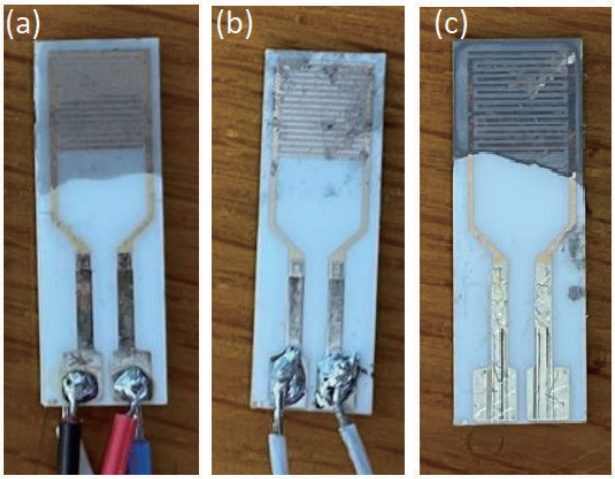

Fig. 1. (Color online) Photographs of films deposited from all three types of graphene dispersions on interdigitated ceramic substrates with gold electrodes: (a) graphene from ultrasonic bath, (b) graphene from ultrasonic probe, and (c) commercially available electrochemical graphene. The width and length of the graphene films are ~1 cm.

and 32 mA was used for this study. Survey spectra from binding energies of 0 to 1000 eV were recorded with a constant pass energy of 40 eV, a step size of 0.5 eV, and a dwell time of 0.2 s in the FAT mode. Detailed spectra for the C 1s peak were recorded with a pass energy of 20 eV, a step size of 0.1 eV, and a dwell time of 2 s in the FAT mode. Spectra were collected with the SpecsLab data analysis software and studied with the CasaXPS software package.

2.3 Humidity sensing

For humidity sensing and respiration monitoring, each of the three graphene films was assembled on a commercially available ceramic substrate with interdigitated gold contacts (Fig. 1). Such sensors were individually inserted in a custom-made chamber made of polytetrafluoroethylene (PTFE). A reference sensor (Honeywell HIH-4000-001) was placed next to the graphene sensor at a distance of ~2 cm. The humidity chamber was equipped with several valves by which gases could be injected and vented. The sensor response to humidity was monitored with a Keysight 34461a digital multimeter (DMM) in the two-terminal resistance mode (Fig. 2). Before the start of the measurement, the chamber was dried with nitrogen (N_2) gas through one of the valves. The lowest RH was ~10%, after which water vapor was injected through a second valve until RH reached a maximum of ~90%, upon which the injection of water vapor was stopped and the chamber was again dried out with N_2. Three cycles of such measurement were repeated. To establish the linearity of the sensor, a repeated stepwise increase in RH was performed.

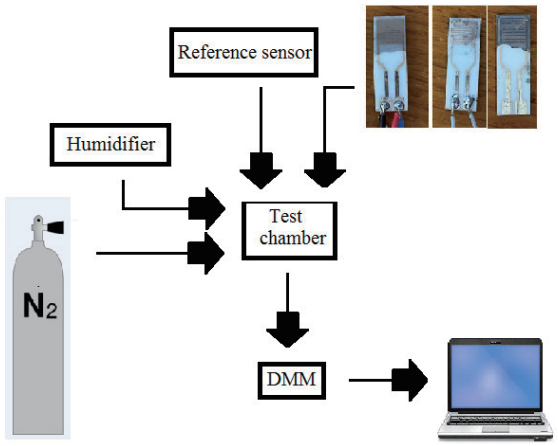

Fig. 2. (Color online) Experimental setup used in this study.

2.4 Respiration monitoring

Respiration monitoring was conducted in a basic experiment under laboratory conditions (temperature ~25 ºC, room humidity ~50% RH). A graphene sensor was placed on a table while a volunteer breathed on the sensor. The sensor responded with a change in resistance. The volunteer breathed at three different paces: fast, normal, and slow.

3. Results and Discussion

3.1 Characterization

Figure 3 depicts the UV–VIS spectrum used to calculate the thickness of each graphene film. The thickness was calculated from the optical transmittance of the film at a wavelength of 660 nm.[4] The graphene film obtained from the dispersion formed with the ultrasonic bath has a transmittance of 77%. Given that one layer of graphene absorbs 2.3% of light at this wavelength, this type of graphene has a thickness of ~3.45 nm (10 graphene layers).[18] The transmittance of the film made from commercial electrochemical graphene is 33%, which indicates a thickness of ~10 nm (29 graphene layers). These two graphene sensors were easily characterized owing to the uniformity of the films [Figs. 1(a) and 1(c)]. The films made from graphene obtained by probe sonication are heterogeneous with different thicknesses in different regions of the film [Fig. 1(b) and inset of Fig. 3]. The transmittance of such a film is 83%, which corresponds to a thickness of 2.55 nm (7.5 graphene layers). Although this thickness was obtained across a large portion of the film, there are also smaller thicker parts, which are visually comparable to the other two graphene films.

Figure 4 shows AFM images from which the average lateral sizes of graphene flakes were determined. Figures 4(a)–4(c) depict the surfaces of graphene obtained by bath sonication, probe

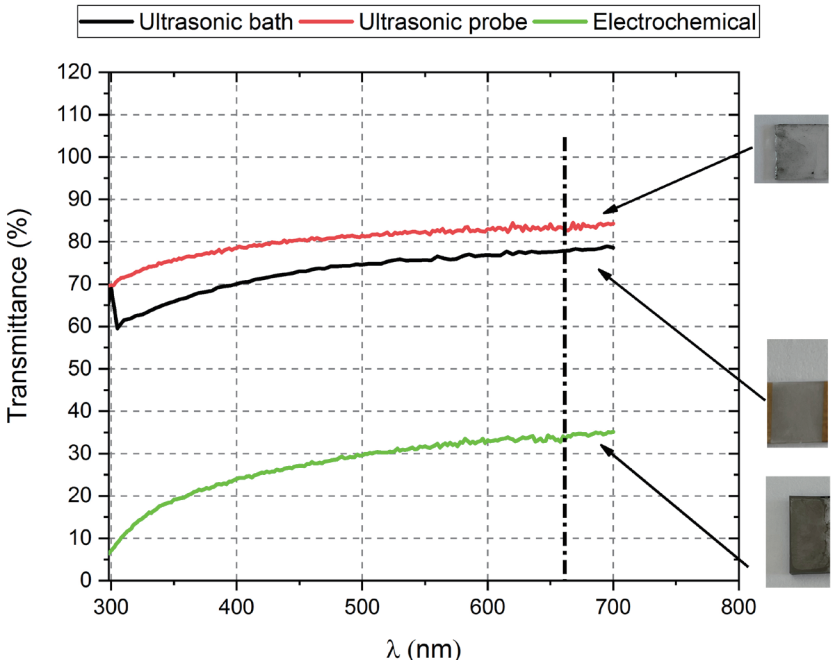

Fig. 3. (Color online) UV–VIS characterization in transmittance mode, by which the thicknesses of the graphene films measured. Insets: photographs of the characterized graphene films. The green, black, and red curves represent the electrochemically exfoliated graphene, bath-sonicated, and probe-sonicated films, respectively.

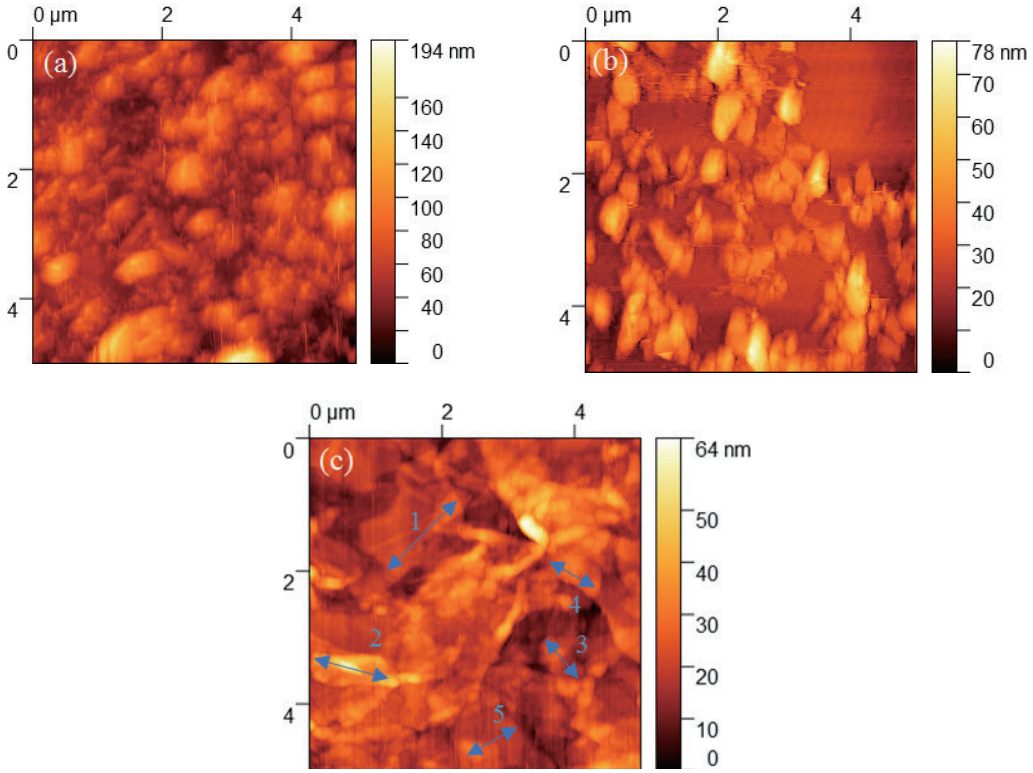

Fig. 4. (Color online) Sample characterization with AFM. Different nanoplatelet sizes are visible in the images: (a) graphene from ultrasonic bath, (b) graphene from ultrasonic probe, and (c) commercially available electrochemical graphene.

sonication, and electrochemical exfoliation, respectively. Lateral sizes were determined by manually measuring the sizes of five random flakes on each image and taking the average. AFM images for graphene obtained by bath and probe sonications [Figs. 4(a) and 4(b)] are easy to interpret, because the flakes are small and have little overlap. Electrochemically exfoliated graphene yields flakes that are larger and have significant overlap; thus, in Fig. 4(c), we show the flakes that we measured, with numbered arrows that correlate with the flake sizes indicated in Table 1. In Table 1, we also provide the average flake sizes for the three exfoliation conditions. Bath sonication yielded an average size of 147 nm, in agreement with the values reported earlier.[15] For comparison, probe sonication yielded flakes that are on average larger (444 nm) but also have a wider size distribution. Electrochemical exfoliation produced the largest flakes, with lateral sizes above 600 nm and reaching ~1500 nm.

Figure 5 illustrates the chemical properties of each graphene film obtained via surveys of XPS spectra. Roughly, all three spectra have similar characteristics but with slight differences.

Table 1
Summary of randomly selected results measured by AFM, extracted from Fig. 4.

	R_1 (nm)	R_2 (nm)	R_3 (nm)	R_4 (nm)	R_5 (nm)	Average size (nm)
Ultrasonic bath	165	117	87	238	126	147
Ultrasonic probe	736	185	287	412	600	444
Commercial electrochemical	1513	1229	847	652	1020	1052

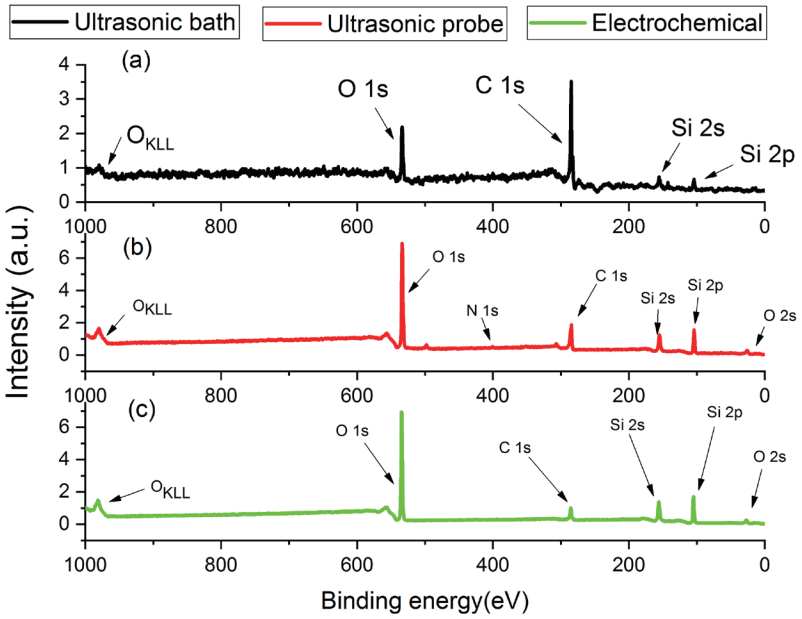

Fig. 5. (Color online) Survey XPS spectra of each graphene: (a) graphene from ultrasonic bath, (b) graphene from ultrasonic probe, and (c) commercially available electrochemical graphene.

All of them show the presence of C, O, and Si (from the substrate) as expected, while in Fig. 5(b), a small peak, which originates from nitrogen appears at approximately 400 eV. The deconvoluted XPS spectrum for C 1s, corresponding to graphene obtained from the ultrasonic bath, has two peaks at 284.9 and 285.2 eV, which correspond to sp^3 and sp^2 hybridizations, respectively, and another peak at 286.4 eV, which corresponds to the C−O bond [Fig. 6(a)].[19] Graphene obtained from the ultrasonic probe has slight shifts of 0.6 and 0.3 eV for the peaks for sp^3 and sp^2 hybridizations, respectively, relative to graphene from the ultrasonic bath, where the C−C bond is located at 284.3 eV and the C=C bond is at 285.5 eV with a O−C=O functional group at 288.8 eV [Fig. 6(b)].[20] This shift can be attributed to different levels of oxidation between the two films. Figure 6(c) represents C 1s peaks for the electrochemically exfoliated graphene. The C−C bond is at 284.5 eV and the C=C bond is at 285.2 eV, while the peak corresponding to the C−O bond is located at 287.1 eV. Figure 6 indicates that the film obtained from graphene exfoliated in an ultrasonic bath has the lowest oxidation. Both the graphene from the ultrasonic probe and the electrochemically exfoliated graphene have higher intensity peaks related to the oxygen bond than graphene from the ultrasonic bath. Their peaks are of similar intensity but with different bond types, as indicated by the 1.7 eV shift in peak position between them. Graphene obtained

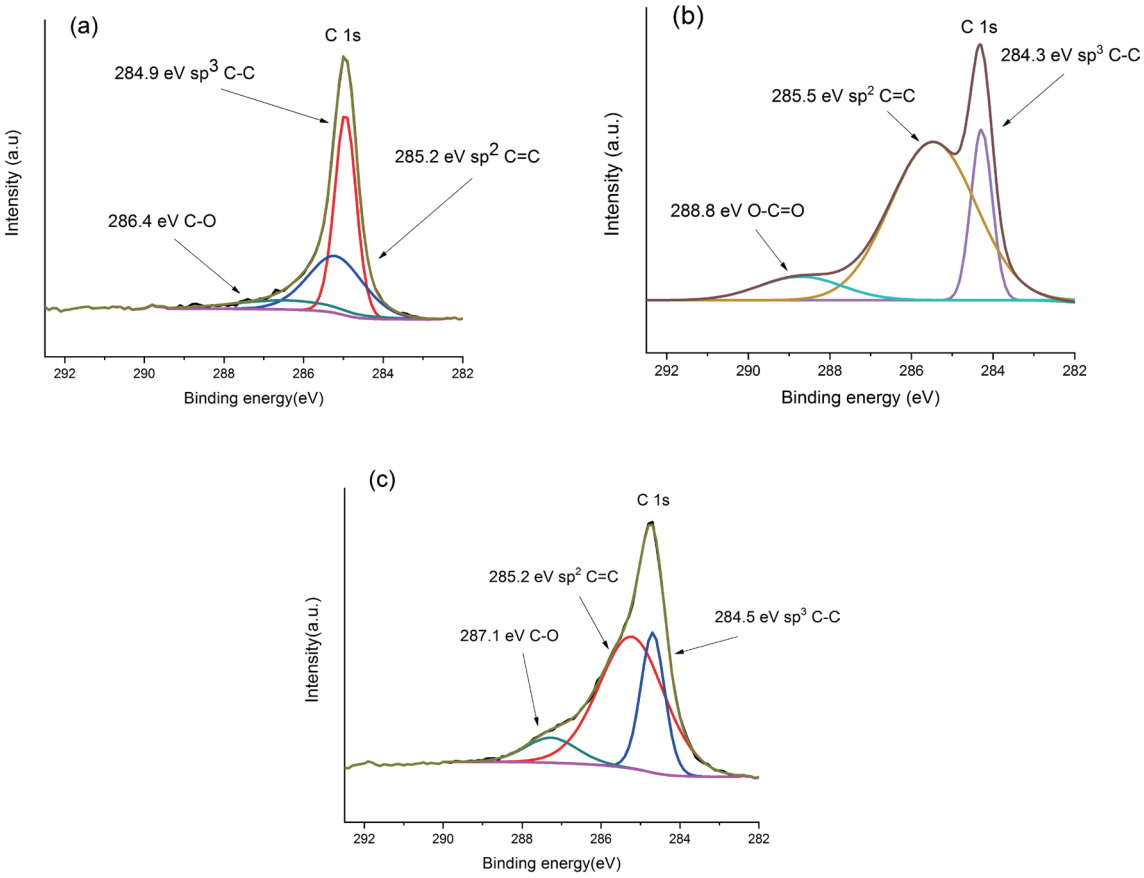

Fig. 6. (Color online) Deconvoluted XPS peaks for C1s for (a) graphene from ultrasonic bath, (b) graphene from ultrasonic probe, and (c) commercially available electrochemical graphene.

from the ultrasonic probe shows a stronger oxidation than graphene from the ultrasonic bath and electrochemically exfoliated graphene, which is distinguished by having an O−C=O group instead of a simple C−O bond, as a result of a complex synthesis process in which several solvents are exchanged.

3.2 Humidity sensing

Figure 7 shows the response of the graphene-based sensors to changes in humidity. The output of the graphene-based sensors was measured in parallel to the output of a reference sensor, which provides the exact RH in the chamber (pink line in Fig. 7). For the starting point, a minimum of ~10% RH was established, and then the humidity was increased to a maximum of ~90% RH in the chamber. The maximum RH was chosen on the basis of the saturation point of the particular graphene sensor, beyond which the resistance did not change significantly. The saturation point for all three sensors occurred at around 90% RH. After reaching the maximum RH, the chamber was cleared out with a blast of nitrogen, which produced a rapid decrease in RH. These steps were repeated in three cycles. All three types of liquid-phase-exfoliated graphene were distinguished by a stable baseline and repeatability. Graphene obtained by bath sonication yielded sensors with the largest baseline drift due to chemisorption [Fig. 7 (a)]. Graphene obtained by probe sonication had the highest inhomogeneity, yielding sensors with the largest noise, as seen in Fig. 7(b). However, the assembled film was ~2.2 nm thick, making it the

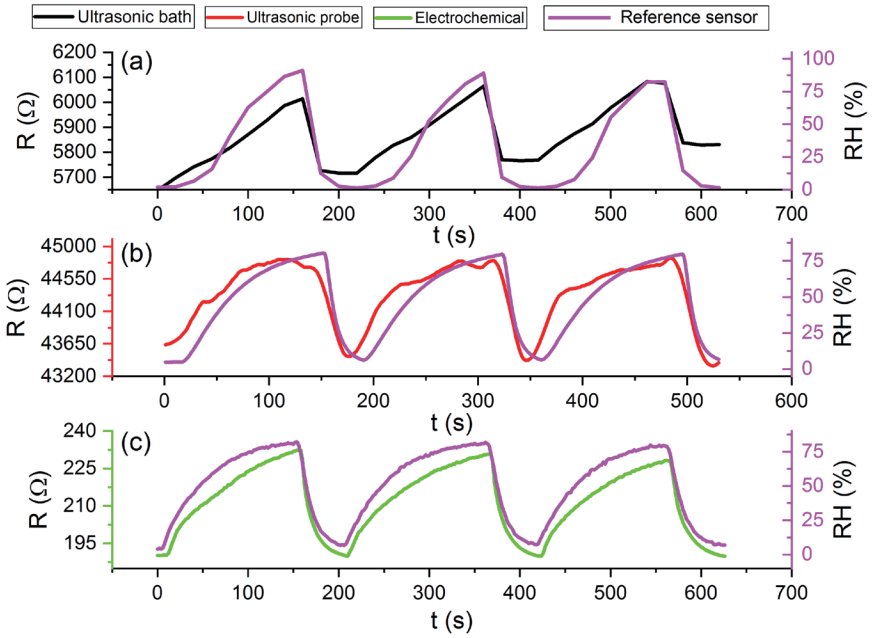

Fig. 7. (Color online) Response over time of graphene sensors to humidity with reference to commercial humidity sensor (Honeywell HIH-4000-001), measured in three cycles from ~10% to ~90% RH: (a) graphene sensor obtained with the ultrasonic bath, (b) graphene sensor obtained with an ultrasonic probe, and (c) sensor fabricated from electrochemically synthesized graphene. In (b), the data has been smoothed for clarity.

thinnest among the three films. Figure 7(c) shows the results obtained from commercially available electrochemically exfoliated graphene. This film had the lowest resistance among the three films, starting at a value below 200 Ω, which is a result of a thickness of ~10 nm. A comparison of the sensitivities of the three different sensors is given in Table 2.

The sensitivity (S) of a chemiresistive gas sensor is given as

$$S = 100 \cdot \frac{\Delta R}{R_0}, \tag{1}$$

where R_0 is the initial resistance and ΔR is the difference between the given resistance and the initial resistance. The most interesting RH range is between 30 and 80%, corresponding to the naturally occurring range of values. Table 2 shows the average sensitivity of each type of graphene sensor in this target range. The average sensitivities are 1% for graphene obtained with an ultrasonic probe, 2.4% for graphene obtained with an ultrasonic bath, and 13.4% for the commercially available electrochemical graphene. The obtained average sensitivity across the RH range is correlated with the graphene thickness, where the thinnest graphene film has the lowest sensitivity and the thickest film has the highest sensitivity. For a clearer view of the graphene sensor performance, a comparison was pursued with the data obtained with different graphene sensor types. Single- and double-layer CVD graphene films show sensitivities of 0.31 and 0.2% respectively, while the thinnest graphene film that comes from an ultrasonic probe has a sensitivity of 1%.[6,21] Electrospray-printed graphene shows a sensitivity up to ~20%, which is higher than that shown in this paper; however, the resistance for such graphene is near 200 kΩ, which is higher than that shown in this paper.[7]

Figure 8 shows the response of each graphene sensor over several cycles of increasing RH in a stepwise manner. The original baseline drift was corrected by linear subtraction to observe the results better. The apparent response and recovery times that could be inferred from these graphs are actually a measure of the chamber filling and purging times, and hence do not represent the response times of the graphene sensor, which are orders of magnitude smaller than the chamber response times. Figure 8(d) depicts the linearity of the relative change in resistance (S) as a function of RH at the maximum value. For a clear view of the linearity, the Pearson correlation coefficient (r) was calculated. The correlation coefficients of the graphene sensors from the ultrasonic bath, ultrasonic probe, and electrochemically exfoliated graphene are r = 0.97653, 0.99129, and 0.99289, respectively. All three sensors have linear behavior with high Pearson correlation coefficient.

Table 2
Percentage change of resistance for each graphene sensor in the range 30–80% for each cycle (ascending path) and average sensitivity. Results taken from Fig. 7.

	Cycle 1 (%)	Cycle 2 (%)	Cycle 3 (%)	Average (%)
Ultrasonic bath	2.6	2.2	2.5	2.4
Ultrasonic probe	1	1	0.9	1
Commercial electrochemical	14	14	12.3	13.4

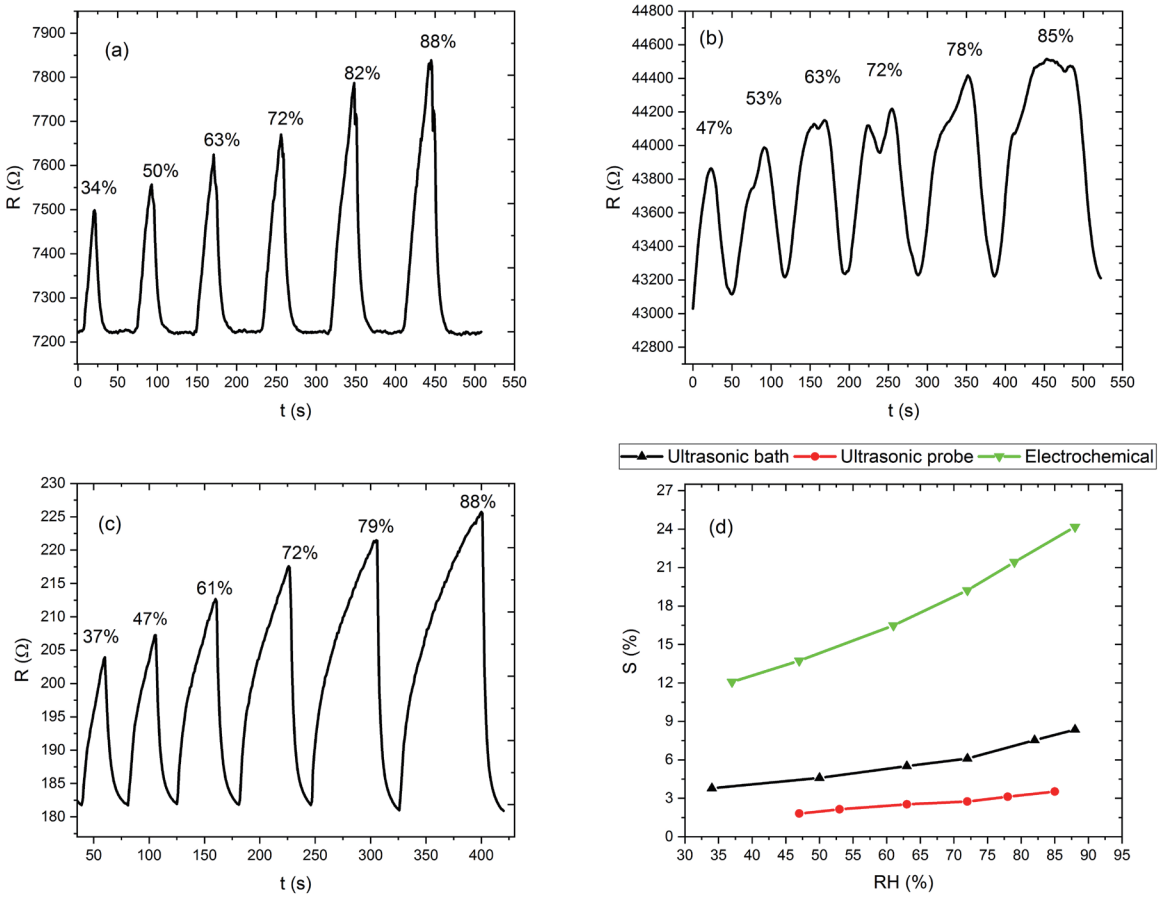

Fig. 8. (Color online) Graphene senor response over time to rapid stepwise increase in RH: (a) sensor output from graphene obtained from an ultrasonic bath, (b) sensor output from graphene obtained with an ultrasonic probe, (c) sensor output from electrochemically synthesized graphene, and (d) peak response as a function of RH for all three graphene sensors. In (b), the data has been smoothed for clarity.

3.3 Respiration monitoring

Ultrafast graphene-based humidity sensors, in addition to determining the static RH, can be used to monitor human inhalation and exhalation, namely, respiration. Figure 9 depicts the results of breathing on each type of graphene sensor at fast, normal, and slow paces. Graphene sensors were placed on a table, and a volunteer exhaled and inhaled directly on each sensor in three cycles at each of the breathing paces. For fast breathing, it can be seen that there is a sharp peak, after which the output returns to the baseline. The signal output for normal breathing is distinguished by plateaus of ~2, ~8, and ~8 s for graphene from the ultrasonic bath, graphene from the ultrasonic probe, and electrochemically exfoliated graphene, respectively. The distinguished plateaus for slow breathing are ~4, ~14, and ~22 s for the three types of graphene, respectively (Fig. 9). All three graphene sensor types show similar trends at different respiration rates, with different time intervals for the plateaus, which are related to the thickness and topography of the individual graphene materials. The usefulness of such sensors for respiration monitoring lies in their practicality of use in a basic experiment, i.e., the sensor is placed on a

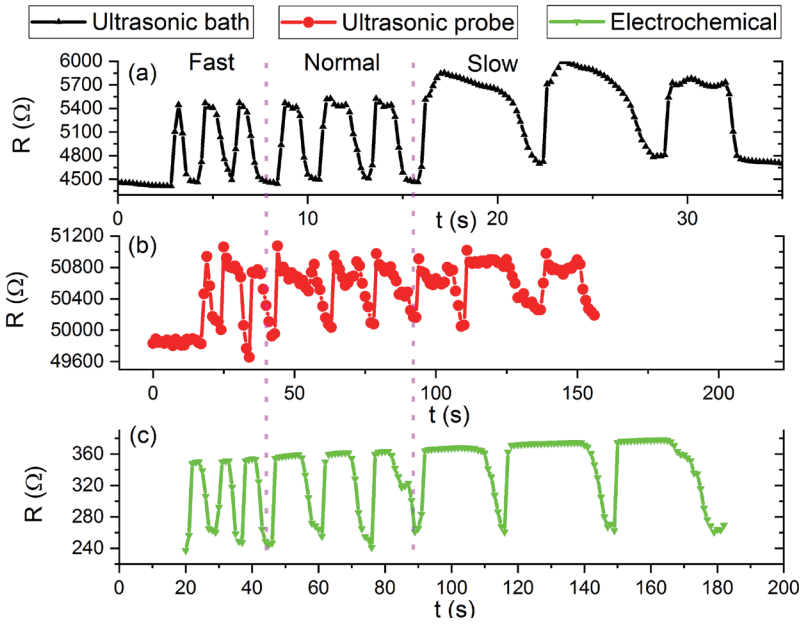

Fig. 9. (Color online) Sensor response over time while monitoring fast, normal, and slow respirations for each graphene sensor: (a) graphene from ultrasonic bath, (b) graphene from ultrasonic probe, and (c) commercially obtained electrochemical graphene.

desk and the volunteer simply takes breaths, directly breathing on the sensor without wearing a mask, showing potential for further applications. The sensitivity is high at values up to ~40% for the commercially obtained graphene.

4. Discussion

The process of obtaining graphene significantly affects the sensor performance owing to differences in film homogeneity, thickness, and functional group, all of which may affect the interaction of the film with water molecules in humid air. There is an evident inverse correlation between the measured film resistance and sensitivity to changes in humidity. The sensor with the lowest resistance has the highest sensitivity, and the sensor with the highest resistance has the lowest sensitivity. Higher resistance stems from the inhomogeneity of some of the films, which consist of islands of materials that do not cover the full sensor area, particularly our films made from probe-sonicated graphene. Since for such films the area covered by graphene is smaller than in the other two cases, the total volume reactive to gas is also smaller, resulting in lower sensitivity. The film made from bath-sonicated graphene is continuous and thinner than that made from electrochemically exfoliated graphene (EEG), but it also consists of smaller flakes (Fig. 3). Although it would be reasonable to expect that a film consisting of smaller flakes is more reactive to gases than that consisting of larger flakes because the former contains a higher density of reactive edge sites,[16,22–24] that made from EEG is more reactive than that made from bath-sonicated graphene. The likely reason for the higher sensitivity is the larger film thickness, which translates to a larger total reaction volume. Thus, in future work on thin-film

gas sensors made from liquid-phase-exfoliated graphene, care should be taken about the trade-off between flake size (edge density) and film thickness (total reactive volume).

5. Conclusion

In this paper, we presented a comparison of three types of graphene humidity sensors, with appropriate characterization that aids in understanding the obtained results. All graphene films were obtained by LPE but exfoliated with different methods, which implies that the obtained graphene films have different characteristics, with different films utilized depending on the application. In contrast to traditional humidity sensors, which have slow response times, graphene-based sensors are fast enough for dynamic applications such as respiration monitoring. We have demonstrated that, regardless of the exfoliation method used, films made from liquid-phase-exfoliated graphene and deposited by LB assembly are robust and useful for sensor applications.

Acknowledgments

The authors would like to thank Dr. Ana Dobrota and Dr. Nemanja Gavrilov from the Faculty of Physical Chemistry, University of Belgrade, Serbia, for both experimental and theoretical advice that greatly contributed to the writing of this paper. This work was supported by the Science Fund of the Republic of Serbia through Project Gramulsen (6057070). We also acknowledge funding from the Ministry of Education, Science, and Technological Development of the Republic of Serbia through grant no. 451-03-68/2022-14/200026. TTI acknowledges funding provided by the Institute of Physics Belgrade, through a grant by the Ministry of Education, Science, and Technological Development of the Republic of Serbia.

References

1 T. A. Blank, L. P. Eksperiandova, and K. N. Belikov: Sens. Actuators, B **228** (2016) 416. https://doi.org/10.1016/j.snb.2016.01.015
2 X. Liu, S. Cheng, H. Liu, S. Hu, D. Zhang, and H. Ning: Sensors **12** (2012) 9635. https://doi.org/10.3390/s120709635
3 A. E. Galashev and O. R. Rakhmanova: Phys-Usp+. **57** (2014) 970. https://doi.org/10.3367/ufne.0184.201410c.1045
4 F. Bonaccorso, Z. Sun, T. Hasan, and A. C. Ferrari: Nat. Photonics **4** (2010) 611. https://doi.org/10.1038/nphoton.2010.186
5 S. Papamatthaiou, D. P. Argyropoulos, F. Farmakis, A. Masurkar, K. Alexandrou, I. Kymissis, and N. Georgoulas: Procedia Eng. **168** (2016) 301. https://doi.org/10.1016/j.proeng.2016.11.201
6 A. D. Smith, K. Elgammal, F. Niklaus, A. Delin, A. C. Fischer, S. Vaziri, F. Forsberg, M. Råsander, H. Hugosson, L. Bergqvist, S. Schröder, S. Kataria, M. Östling, and M. C. Lemme: Nanoscale **7** (2015) 19099. https://doi.org/10.1039/c5nr06038a
7 A. P. Taylor and L. F. Velásquez-García: Nanotechnology **26** (2015) 505301. https://doi.org/10.1088/0957-4484/26/50/505301
8 S. Borini, R. White, D. Wei, M. Astley, S. Haque, E. Spigone, N. Harris, J. Kivioja, and T. Ryhänen: ACS Nano **7** (2013) 11166. https://doi.org/10.1021/nn404889b
9 B. Jiang, Z. Bi, Z. Hao, Q. Yuan, D. Feng, K. Zhou, L. Zhang, X. Gan, and J. Zhao: Sens. Actuators, B **293** (2019) 336. https://doi.org/10.1016/j.snb.2019.05.024
10 C. Backes, T. M. Higgins, A. Kelly, C. Boland, A. Harvey, D. Hanlon, and J. N. Coleman: Chem. Mater. **29** (2017) 243. https://doi.org/10.1021/acs.chemmater.6b03335

11 S. Witomska, T. Leydecker, A. Ciesielski, and P. Samorì: Adv. Funct. Mater. **29** (2019) 1901126. https://doi.org/10.1002/adfm.201901126
12 H. Kim, C. Mattevi, H. J. Kim, A. Mittal, K. A. Mkhoyan, R. E. Riman, and M. Chhowalla: Nanoscale **5** (2013) 12365. https://doi.org/10.1039/c3nr02907g
13 S. Andrić, T. Tomasevic-Ilic, M. Bošković, M. Sarajlić, D. Vasiljević-Radović, M. M. Smiljanic, and M. Spasenović: Nanotechnology **32** (2020) 025505. https://doi.org/10.1088/1361-6528/abb973
14 F. Vasileva, V. Popov, I. Antonova, and S. Smagulova: Materials **15** (2022) 1256. https://doi.org/10.3390/ma15031256
15 A. Matković, I. Milošević, M. Milićević, T. Tomašević-Ilić, J. Pešić, M. Musić, M. Spasenović, D. Jovanović, B. Vasić, C. Deeks, R. Panajotović, M. R. Belić, and R. Gajić: 2D Mater. **3** (2016) 015002. https://doi.org/10.1088/2053-1583/3/1/015002
16 T. Tomašević-Ilić, Đ. Jovanović, I. Popov, R. Fandan, J. Pedrós, M. Spasenović, and R. Gajić: Appl. Surf. Sci. **458** (2018) 446. https://doi.org/10.1016/j.apsusc.2018.07.111
17 T. Tomašević-Ilić, J. Pešić, I. Milošević, J. Vujin, A. Matković, M. Spasenović, and R. Gajić: Opt. Quant. Electron. **48** (2016) 319. https://doi.org/10.1007/s11082-016-0591-1
18 R. R. Nair, P. Blake, A. N. Grigorenko, K. S. Novoselov, T. J. Booth, T. Stauber, N. M. R. Peres, and A. K. Geim: Science **320** (2008) 1308. https://doi.org/10.1126/science.1156965
19 L. Rakočević, I. Srejić, A. Maksić, J. Golubović, and S. Štrbac: Catalysts **11** (2021) 481. https://doi.org/10.3390/catal11040481
20 L. Rakočević, I. S. Simatović, A. Maksić, V. Rajić, S. Štrbac, and I. Srejić: Catalysts **12** (2022) 43. https://doi.org/10.3390/catal12010043
21 X. Fan, K. Elgammal, A. D. Smith, M. Östling, A. Delin, M. C. Lemme, and F. Niklaus: Carbon **127** (2018) 576. https://doi.org/10.1016/j.carbon.2017.11.038
22 Y. Yang and R. Murali: Phys. Lett. **98** (2011) 2011. https://doi.org/10.1063/1.3562317
23 G. C. Mastrapa and F. L. Freire: J. Sens. **2019** (2019). https://doi.org/10.1155/2019/5492583
24 M. Spasenovic, S. Andric, and T. Tomasevic-Ilic: Proc.2021 IEEE 32nd Int.l Conf. Microelectronics (IEEE, 2021) 25–28. https://doi.org/10.1109/MIEL52794.2021.9569192

About the Authors

Stevan Andrić received his B.S. degree at the Faculty of Physical Chemistry, University of Belgrade, Serbia in 2017 and his M.S. degree in 2018 also at the Faculty of Physical Chemistry, University of Belgrade. He is currently working at the Department of Microelectronic Technologies, Institute of Chemistry, Technology and Metallurgy, University of Belgrade, where he is pursuing his Ph.D. degree at the Faculty of Physical Chemistry. His research fields are in 2D materials, their exfoliation and application, gas sensors, motion detection sensors, and the electrochemical characterization of materials. (stevan@nanosys.ihtm.bg.ac.rs)

Tijana Tomašević-Ilić is a research associate at the Institute of Physics Belgrade, University of Belgrade. She obtained her Ph.D. in physical chemistry from the Faculty of Physical Chemistry, University of Belgrade in September 2019. Her work in the Laboratory for 2D Materials is focused on the liquid-phase exfoliation of layered, 2D nanomaterials, the controlled deposition of nanomaterials into thin films, the functionalization/surface modification of 2D materials by various covalent and noncovalent strategies, and the investigation of 2D material-based thin-film applications (e.g., FETs, sensors, and protective coatings). (ttijana@ipb.ac.rs)

Lazar Rakočević received his B.S. and M.S. degrees from the Faculty of Physical Chemistry, University of Belgrade, Serbia, in 2018 and 2019, respectively. He is currently pursuing his Ph.D. degree at the Faculty of Physical Chemistry, University of Belgrade. His research interests are in electrochemistry, catalysis, materials, and X-ray photoelectron spectroscopy. (lazar.rakocevic@vin.bg.ac.rs)

Dana Vasiljević Radović received her B.S. degree in electrical engineering from the School of Electrical Engineering, University of Belgrade in 1991 and her M.S. and Ph.D. degrees in material science from the University of Belgrade in 1995 and 1997, repectively. Currently, she is a full research professor and the head of the Department of Microelectronic Technologies, Institute of Chemistry, Technology and Metallurgy, University of Belgrade. Her main areas of expertise are the research and development of micro/nanosystem (MEMS and NEMS)-based sensors, detectors, and actuators, and also the AFM characterization of materials and MEMS/NEMS components. (dana@nanosys.ihtm.bg.ac.rs)

Marko Spasenović received his B.Eng. (engineering physics) from Carleton University in Ottawa, Canada, in 2005 and his M.S. in physics from the University of Toronto, Canada, in 2006. He received his Ph.D. degree in applied physics from the University of Twente and AMOLF in the Netherlands in 2011. From 2011 to 2014, he was a postdoctoral researcher at the Institute for Photonic Sciences (ICFO) near Barcelona, Spain. From 2014 to 2018, he was at the Institute of Physics in Belgrade, Serbia, where he held the positions of assistant research professor and associate research professor. Since 2018, he has been with the Institute of Chemistry, Technology and Metallurgy in Belgrade, Serbia, where he is an associate research professor. His research interests include the use of graphene and other 2D materials for sensing, particularly as gas sensors, physiological parameter sensors, and acoustic transducers. (spasenovic@nanosys.ihtm.bg.ac.rs)